Quantitative Image Analysis of Laser-induced Choroidal Neovascularization in Rat

JEFFREY L. EDELMAN* AND MARISOL R. CASTRO

Department of Biological Sciences, Allergan Inc., Irvine, CA, U.S.A.

Rodent models of laser-induced choroidal neovascularization (CNV) are now extensively used to identify angiogenic proteins, determine the role of specific genes with knockout mice, and evaluate the efficacy and safety of anti-angiogenic therapies. CNV is typically evaluated by fluorescein angiography or vascular endothelial cell labeling in histologic sections. The current study examined an alternative method using high molecular weight FITC-dextran (MW 2×10^6) for high resolution angiography in RPE-choroid-sclera flat mounts. At 24 hr after lasering, the lesions appeared as a circular weakly fluorescent area of approximately equal diameter to the laser spot. No FITC-dextran labeled blood vessels were visible in the lesion at day 1. Three days after lasering, 47 % of the lesions showed FITC-dextran labeling indicative of CNV. The incidence (71 %) and extent of CNV increased by day 6, and by day 10 all lesions were vascularized, and the maximal area was attained. No significant change followed day 10, and the neovascular area remained constant through day 31. The highest rate of blood vessel growth (between 3 and 10 days after laser) correlates with the peak expression of VEGF, bFGF, and their receptors shown in previous studies. Morphologic analysis of flat mounts and histologic sections showed that the neovascular plexus in most lesions originates from deeper choroidal vessels in the center of the lesion, grows towards the neural retina, then branches circumferentially to anastamose with uninjured choriocapillaris. The microvessels in these lesions are broad and flat, similar to normal choriocapillaris. In a separate study, rats were treated daily with the angiostatic corticosteroid dexamethasone (20–500 μg kg^{-1} day^{-1}), and CNV was examined at day 10 in FITC-dextran labeled flat mounts and histologic sections. Dexamethasone dose-dependently inhibited CNV, and its highest dose inhibited approximately 95 % of CNV labeled by FITC-dextran and resulted in lesions with no detectable Factor VIII immunostaining. High resolution angiography with FITC-dextran is reproducible and quantifiable, and it may accelerate the discovery of therapeutic agents that modulate choroidal neovascularization.

© 2000 Academic Press

Key words: angiogenesis; neovascularization; chorocapillaris; corticosteroids; laser.

1. Introduction

The protein extravasation and hemorrhage associated with choroidal neovascularization (CNV) are primary causes of severe vision loss in retinal diseases such as age-related macular degeneration (ARMD) (D'Amico, 1994; Lee, Wang and Adamis, 1998). In ARMD, the normal barrier function of Bruch's membrane is compromised, and CNV can develop either under the retinal pigment epithelium (RPE) or within the subretinal space between RPE and photoreceptor outer segments. Recent experimental and clinical efforts have focused on developing therapeutic strategies for exudative ARMD that either obstruct perfusion or inhibit the growth of new choroidal blood vessels (Miller et al., 1995; Seo et al., 1999). As novel anti-angiogenic therapies become available, animal models of CNV are required to evaluate their local and systemic toxicity and efficacy.

An established model of CNV is laser photocoagulation of the RPE and choroid in primates (Ryan, 1979)

and rodents (Dobi, Puliafito and Destro, 1989; Frank, Das and Weber, 1989; Seo et al., 1999). Laser photocoagulation selectively ablates the photoreceptor outer segments, RPE, choriocapillaris, and portions of the anterior choroid. The subsequent wound response includes the ingrowth of fibroblasts, RPE, and vascular endothelial cells that form a defined neovascular lesion. Previous studies have characterized these infiltrating cell types and have identified the expression of vascular endothelial growth factor, fibroblast growth factor, and other proteins typically associated with new blood vessel growth (Nishimura et al., 1990; Zhang, Samadani and Frank, 1993; Ishibashi et al., 1995, 1997; Ogata et al., 1996, 1997; Yi et al., 1996). Tobe et al. (1998) showed that basic fibroblast growth factor was not required for laser-induced CNV in knockout mice lacking this angiogenic protein.

Laser-induced CNV has also been used to evaluate inhibitors of angiogenesis in rodents (Seo et al., 1999; Takehana et al., 1999) and to evaluate photodynamic therapy in primates (Miller et al., 1995). The predominant methods of determining efficacy in these studies and in knockout mice are fluorescein

---

* Address correspondence to: Jeffrey L. Edelman, Allergan Inc., 2525 Dupont Dr., Irvine, CA 92612, U.S.A. E-mail: edelman_jeffrey@allergan.com

angiography and histology using serial cross sections. Both of these methods have technical limitations. Conventional fluorescein angiography is not amenable to high resolution analysis and is not easily quantified. Furthermore, the relationship between blood vessel growth, vascular permeability, and fluorescein leakage in these models has not been carefully studied. Histologic analysis of CNV is commonly used, but adequate sampling of histologic sections and quantifying blood vessel growth is technically difficult and extremely labor intensive (Seo et al., 1999). A method that readily measures experimental CNV with high resolution would accelerate the discovery of genes and anti-angiogenic therapies that modulate choroidal neovascularization.

Fluorescein isothiocyanate (FITC)-dextrans of high molecular weight (MW 2×10^6) are retained within blood vessels after fixation and can be used to label vascular volume (D'Amato, Wesolowski and Smith, 1993; Smith et al., 1994). This method of high resolution angiography was used to measure blood vessel growth in retinal flat mounts from a mouse model of oxygen-induced retinopathy (Smith et al., 1994). Similar to retinal vessel growth in mouse, the newly formed choroidal vessels in the rat laser model of CNV grow roughly parallel to the retinal layers and RPE (Dobi et al., 1989). Therefore, high resolution angiography may also be applied to visualizing CNV in RPE-choroid flat mounts. The goals of the current study were to validate this method, to establish the temporal and spatial growth of CNV after lasering, and to compare the effect of an angiostatic compound on CNV in FITC-dextran flat mounts and histologic cross sections.

2. Materials and Methods

Argon Laser-induced CNV in Rats

All animal studies conformed to the ARVO Statement for the Use of Animals in Ophthalmic and Vision Research, and they were approved by the Animal Care Committee at Allergan. To induce choroidal neovascularization, male Brown Norway rats weighing between 200 and 300 g were anesthetized by intramuscular injection of ketamine (100 mg kg^{-1}) and xylazine (10 mg kg^{-1}), and both pupils were dilated with 1 % Tropicamide. Celluvisc (Allergan Inc., Irvine, CA, U.S.A.) was applied to each eye, and a glass coverslip was placed orthogonal to the visual axis. The retina was viewed through a slit lamp microscope, and the optic nerve head was centered into the microscope field. Both eyes received 3 or 4 laser burns between retinal vessels around the optic nerve head using the blue-green setting of a Coherent Novus 2000 Argon Laser (Coherent, Inc., Santa Clara, CA, U.S.A.). The laser power was 90 mW for 100 ms, and the spot diameter was 100 μm. In drug studies, the test group received dexamethasone (Sigma, St. Louis,

MO, U.S.A.) in approximately 1 ml corn oil once daily by oral gavage, and the control group received corn oil only.

Visualizing and Quantifying CNV using FITC-dextran Labeling

Blood vessels were labeled by vascular perfusion with high molecular weight fluorescein isothiocyanate (FITC)-dextran (2×10^6 MW; Sigma, St. Louis, MO, U.S.A.) by a method similar to that described previously (D'Amato et al., 1993). Rats were killed with 100% CO$_2$, and approximately 50 ml of lactated Ringer was injected via the left ventricle, followed by 20 ml of 10% gelatin with 5 mg ml^{-1} of FITC-dextran in lactated Ringer. The eyes were cooled by aerosol refrigerant and stored in 10% formalin. RPE-choroid-sclera flat mounts were obtained by hemisecting the eye and peeling the neural retina away from the underlying RPE. Four radial cuts allowed the eyecup to be laid flat onto a microscope slide with the RPE-side facing up. Flat mounts were dehydrated in ETOH followed by xylene.

Flat mounts were visualized using the $20\times$ objective of an epifluorescent compound microscope fitted with the appropriate excitation and emission filters (Nikon Eclipse E600; A. G. Heinze, Irvine, CA, U.S.A.). Images of the neovascular lesions were captured using an analog video camera (MTI 3CCD; A. G. Heinze, Irvine, CA, U.S.A.) coupled to a PC with image capture and analysis software (Image Pro 3.0, Media Cybernetics, Silver Spring, MD, U.S.A.). A calibration image was also obtained from a slide with a grating of known size. Blood vessels within the neovascular lesion that were labeled with FITC-dextran (i.e. hyperfluorescent) were highlighted, and this reproduction of the CNV was converted into a binary (black and white) image. The area (in μm^2) occupied by white pixels was measured and it is presented as 'neovascular area'. The measurements of neovascular area obtained from multiple lesions from both eyes for each animal were averaged.

Histologic Analysis of Paraffin-embedded Cross Sections

Paraffin-embedded cross sections through lesions were examined using Hematoxylin/eosin (H & E) staining and Factor VIII immunostaining of vascular endothelial cells. Eyes were fixed by perfusing 50 ml lactated Ringer and 20 ml of 4 % paraformaldehyde in phosphate-buffered saline via the left ventricle, followed by enucleation and storage of eyes overnight in 4 % paraformaldehyde. The posterior eye cup (retina-RPE-choroid-sclera) was embedded in paraffin, and serial sections 10 μm thick were cut and used for either H & E or immunostaining. Immunostaining for Factor VIII used the rabbit polyclonal IgG antibody specific for human Factor VIII (Dako Corp., Carpinteria, CA, U.S.A.). After incubation with
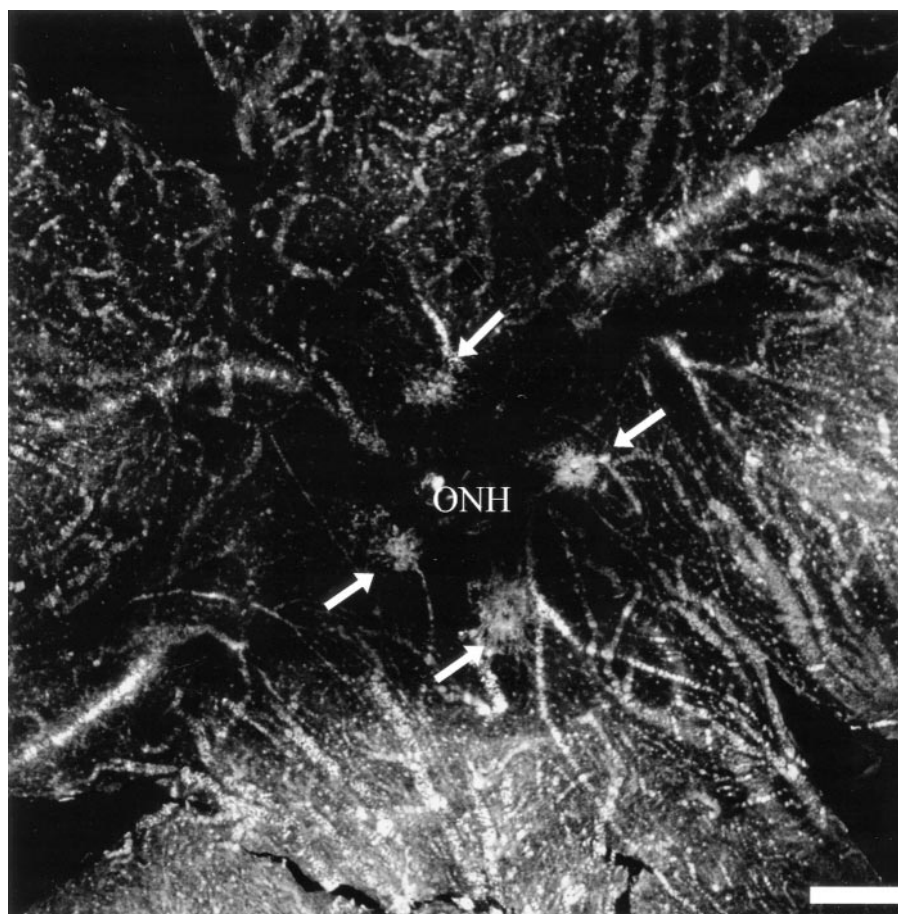
FIG. 1. Low magnification image of CNV in RPE-choroid-sclera flat mount. The vasculature was labeled with 2×10^6 MW FITC-dextran (5 mg ml^{-1}) via cardiac perfusion in rats 10 days after argon laser photocoagulation. Shown is a representative fluorescent image of four laser lesions (arrows) around the optic nerve head (ONH). The bar is 500 μm in length.

primary antibody, sections were stained using a method of horseradish peroxidase streptavidin biotin immunohistochemistry. Normal non-immune rabbit IgG was used as control for staining specificity. Bound immunocomplexes were visualized with amino-ethylcarbazole substrate chromagen (Dako). Sections were counterstained with Mayer's hematoxylin.

Statistical Analysis

All data are presented as mean $\pm$ S.D. with a minimum of three independent measurements unless otherwise noted. Statistical significance was determined using a one-tailed unpaired t-test or Bonferroni multiple comparison analysis. P values $\leqslant 0.05$ are considered statistically significant.

3. Results

Angiographic Analysis of RPE-choroid-sclera Flat Mounts

Laser photocoagulation of the RPE-choroid results in experimental choroidal neovascularization (CNV) which has been characterized by in vivo angiography, histology and vascular casting (Ryan, 1979; Ohkuma and Ryan, 1983; Dobi et al., 1989; Frank et al., 1989; Miller et al., 1990). In the current study, FITC-dextran was used to label blood vessel lumen, and RPE-choroid-sclera flat mounts were examined by fluorescence microscopy to temporally follow experimental CNV after argon laser photocoagulation.

Figs 1 and 2 show low and high magnification images of FITC-dextran-labeled flat mounts. The low magnification image (Fig. 1) shows that CNV in lesions around the optic nerve head appears hyperfluorescent compared to the surrounding choroid which is masked by highly melinated RPE cells and choroidal melanocytes. Fig. 2 shows images obtained with higher magnification fluorescence microscopy of lesions between 24 hr and 31 days after lasering. At 24 hr [Fig. 2(A)], the lesion shows a circular area of weak hyperfluorescence with a diameter approximately equal to that of the laser spot (100 μm). This fluorescence in probably due to a combination of autofluorescence from blood breakdown products, and fluorescence emanating from the underlying sclera where the RPE and choroid have been thermally ablated. No FITC-dextran labeled blood vessels are visible in the lesion at day 1 ($n = 7$, 29 lesions).
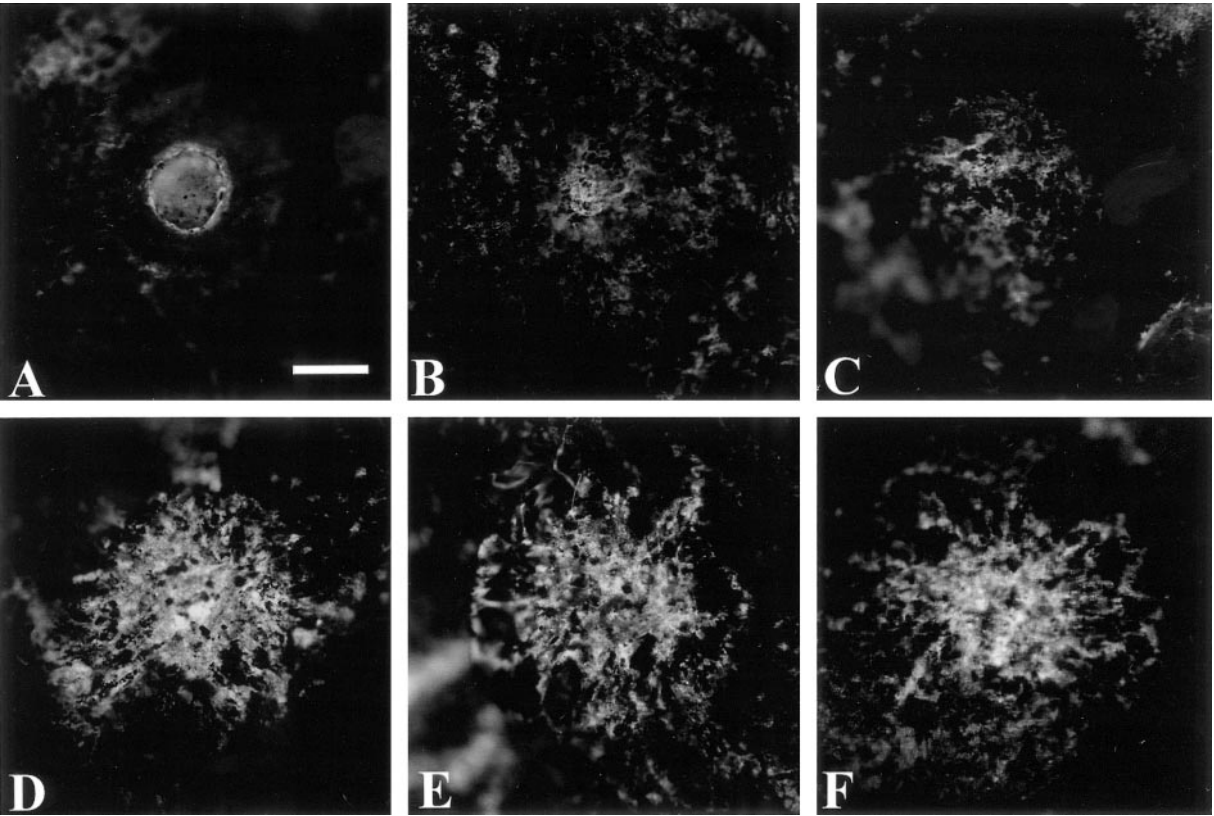
FIG. 2. Higher magnification images of CNV in RPE-choroid-sclera flat mounts. The vasculature was labeled with FITC-dextran via cardiac perfusion 1 day (A), 3 days (B), 6 days (C), 10 days (D), 17 days (E), and 31 days (F) after argon laser photocoagulation. The bar in (A) is 100 μm in length.

At day 3, 16/30 lesions (53 %; $n = 7$) are hypo-fluorescent with no visible new vessel growth; however, 14/30 lesions (47 %) contain FITC-labeled blood vessels primarily in the lesion's center [Fig. 2(B)]. By day 6, the proportion of lesions showing new vessel growth increases to 71 % (20/28; $n = 7$), and the extent of neovascularization also increases [Fig. 2(C)]. At this time, CNV is only observed in the center of the lesion and is usually associated with pigment-laden cells, presumably macrophages. This suggests that CNV originates from deep choroidal vessels that are masked by choroidal melanocytes. The extent and incidence of neovascular labeling both increase dramatically between days 6 and 10. All lesions at day 10 are vascularized (32/32; $n = 7$), and most show a network of broad, flat microvessels, reminiscent of choriocapillaris, that span a circular area approximately 300 μm in diameter [Fig. 2(D)]. The neovascular network at day 17 (33/33 lesions; $n = 7$) and day 31 (22/22 lesions; $n = 4$) appears similar to that of day 10.

All lesions from days 3 to 31 were examined by computer-assisted digital image analysis to measure the area of FITC-dextran-labeled choroidal neovascu-larization. These data are shown graphically in Fig. 3. Neovascular area increases from $3\cdot5 \pm 1\cdot8 \times 10^3$ to $12\cdot0 \pm 7\cdot7 \times 10^3$ μm^2 between days 3 and 6. Between days 6 and 10, neovascular area more than doubles to $28\cdot4 \pm 8\cdot2 \times 10^3$ μm^2. No significant
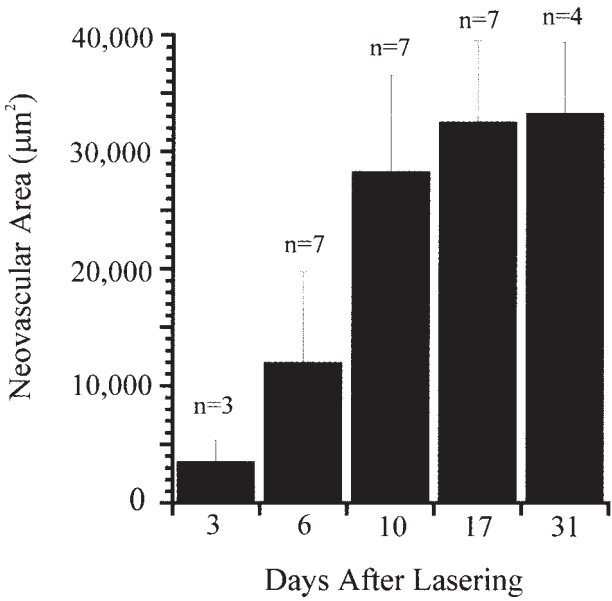

FIG. 3. Time course of neovascular area measured by digital image analysis. Shown is the neovascular area in μm^2 (mean $\pm$ S.D.) for each time point from lesions 3–31 days after argon laser photocoagulation. The number of rats examined in each group is denoted as n. For each rat, 3–7 lesions were averaged. There is no significant difference between days 3 and 6 ($P > 0\cdot05$). Neovascular area at days 3 and 6 is significantly different from that at days 10, 17 and 31 ($P < 0\cdot05$; Bonferroni multiple comparison analysis).
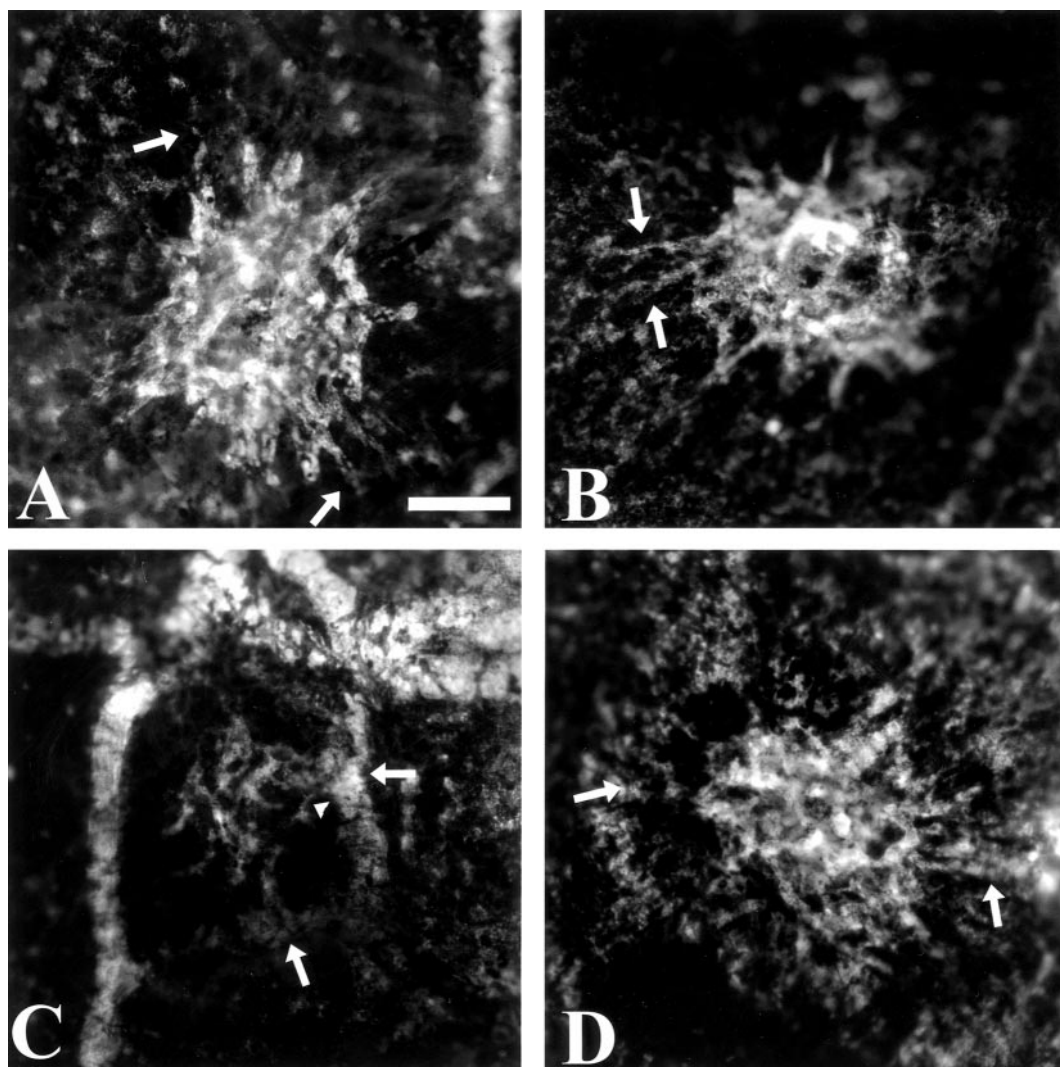
Fig. 4. Representative images of CNV in flat mounts 10 days after lasering. (A, B, D) The most common neovascular nets have broad, flat microvessels that lie anterior to the RPE and anastamose with uninjured choriocapillaris via vessels approximately 10 μm in diameter (arrows). (C) A less common lesion type with small caliber vessels (4·5 μm diameter, arrowhead) that develop deeper in the choroid and are connected to larger choroidal vessels, presumably venules (large arrows). The bar in (A) is 100 μm.

change follows day 10, and the neovascular area is $32\cdot6 \pm 7\cdot0 \times 10^3$ μm^2 at day 17, and $33\cdot4 \pm 6\cdot1 \times 10^3$ μm^2 at day 31.
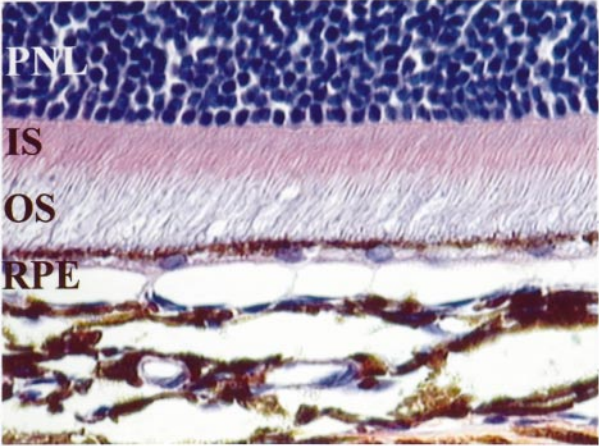
Ten days after lasering, the majority of lesions contain a dense microvascular network that grows anterior to the RPE, resembles the broad flat vessels of normal choriocapillaris, and anastamoses with uninjured choriocapillaris via small caliber vessels which are approximately 10 μm in diameter [Fig. 4(A), (B) and (D)]. In contrast, some neovascular nets are formed by sparse, smaller caliber microvessels derived from larger caliber deep choroidal vessels (40–50 μm) [Fig. 4(C)]. The smallest measurable microvessels in these lesions are $\leqslant 4\cdot5$ μm in diameter.

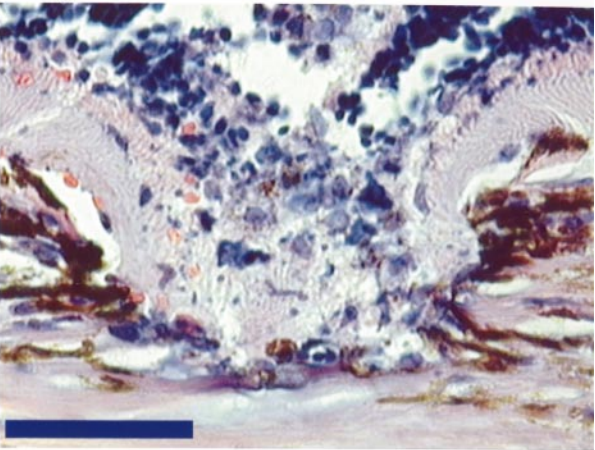*H & E and Factor VIII Immunostaining of Histologic Sections*

Studies were conducted to examine more carefully the relationship between the temporal formation of

FITC-dextran labeled blood vessels in flat mounts and vascular endothelial cell and blood vessel development in histologic sections. Fig. 5 shows representative H & E-stained sections from normal retina-RPE-choroid and from lesions 2 hr to 17 days after lasering. At 24 hr after lasering, photoreceptor outer segments, RPE, and choroid have been thermally ablated, and the extent of this damage has approximately the same diameter as the laser spot (100 μm). The laser energy is absorbed primarily by photoreceptor pigment and by melanin in the RPE apical processes and choroid. No new blood vessels are present at this time. At day 3, a fusiform-shaped lesion has developed that consists primarily of pigment-laden cells, fibroblasts, vascular endothelial cells, and RPE (Zhang et al., 1993). None of the sections examined showed blood vessel formation at day 3. In contrast, blood vessels with red blood cells are seen in the lesion by day 6. At days 10 and 17, the lesion
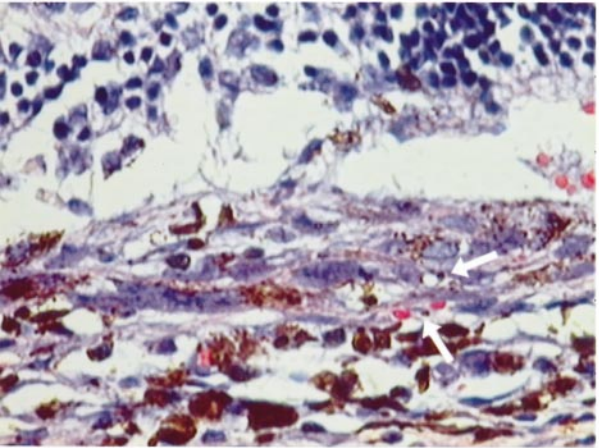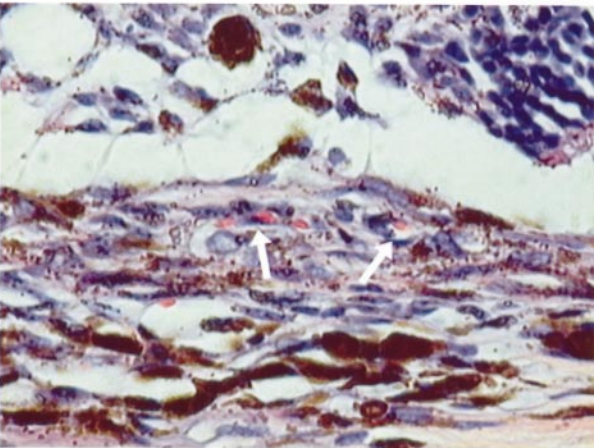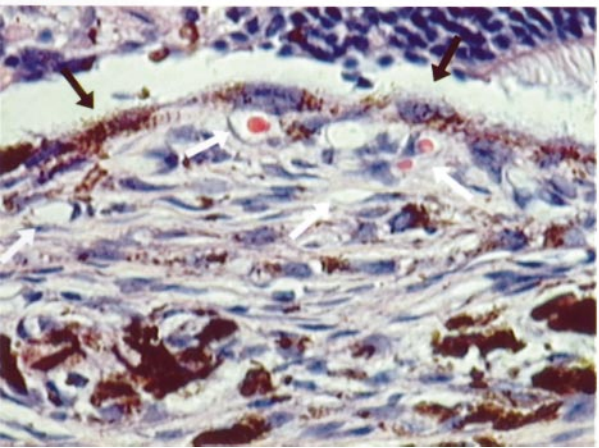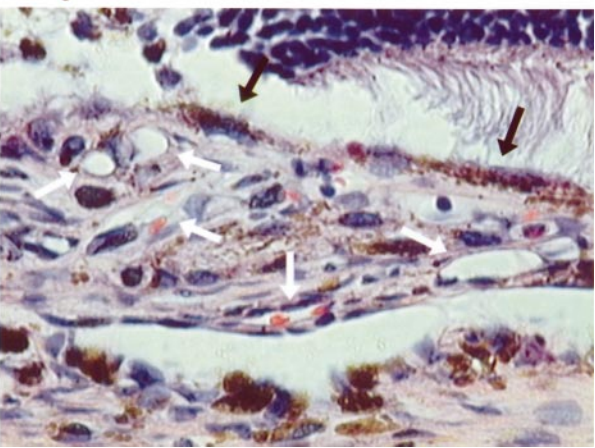
FIG. 5. Hematoxylin and eosin staining of paraffin-embedded cross-sections through choroidal neovascular lesions. Representative images of normal retina-RPE-choroid and images from lesions between days 1 and 17 after argon laser photocoagulation are shown. The white arrows in images from days 3, 6, 10 and 17 denote blood vessels, some of which contain red blood cells within their lumen. The black arrows denote RPE cells that grow over the inner portion of the lesion at days 10 and 17. Shown in normal retina is the photoreceptor nuclear layer (PNL), photoreceptor inner (IS) and outer (OS) segments, and retinal pigment epithelium (RPE). The bar located in the lower left corner of the day 1 image is 50 μm in length. Each image is representative of sections obtained from a minimum of two lesions from two rats.
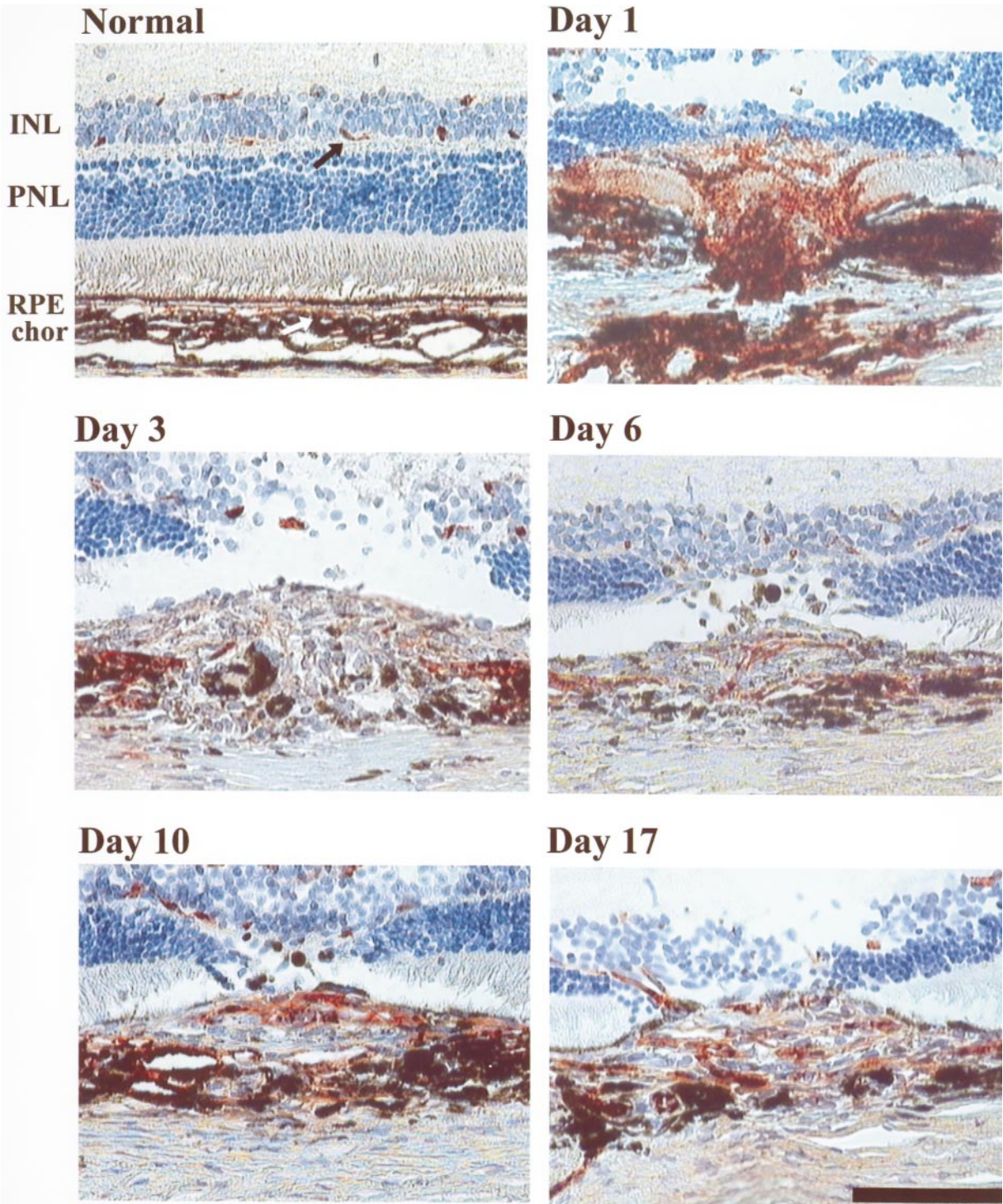
Fɪɢ. 6. Time course of Factor VIII immunostaining after argon laser photocoagulation. Representative images of paraffin-embedded cross sections through normal tissue and those obtained 1, 3, 6, 10 and 17 days after lasering are shown. Factor VIII is labeled with an AEC substrate chromagen which gives a red product. Untreated (normal) eyes show strong Factor VIII staining in the neural retina (black arrow) and choriocapillaris (white arrow). The black bar located in the lower right corner of the day 17 image is 100 μm in length. Each image is representative of sections obtained from a minimum of two lesions from two rats. INL, inner nuclear layer; PNL, photoreceptor nuclear layer; RPE, retinal pigment epithelium; chor, choroid.

height and width has increased, and an RPE monolayer has formed and separated the neural retina from the underlying lesion. All sections examined at these later time points showed more extensive blood vessel formation.

Factor VIII immunostaining was used to specifically follow the progression of vascular endothelial cell invasion into the lesion and subsequent blood vessel formation. Fig. 6 shows immunostained paraffin-embedded cross sections of lesions between 1 and 17 days after lasering. In normal retina, Factor VIII staining is restricted to endothelial cells of large blood vessels (not shown) and microvessels of the neural retina and choriocapillaris. At 24 hr after lasering,

strong Factor VIII staining is seen at the primary site of laser injury and in the surrounding neural retina, choroid, and scleral vessels. Factor VIII is secreted around wounds as a component of the blood clotting cascade. By day 3, strong staining is observed in the choriocapillaris at the periphery of the lesion. Weaker but discrete immunostaining is observed within the lesion, and this suggests the presence of invading vascular endothelial cells. By day 6, Factor VIII-stained endothelial cells form vessels originating from deeper choroidal vasculature. Consistent with the conclusion stated above from fluorescence labeling, this image shows a blood vessel derived from deeper choroid that spans the lesion's center radially and branches outward toward the uninjured choriocapillaris [compared with Fig. 2(C)]. At days 10 and 17, there is an increase in the number and size of Factor VIII-stained vessels within the lesion.

These histologic data show that vascular endothelial cells invade the lesion by day 3 and form functional blood vessels by day 6. The spatiotemporal development of CNV seen in histologic sections is consistent with that seen in FITC-dextran labeled flat mounts (Figs 2 and 3).

Inhibition of Experimental CNV by Dexamethasone

To test the utility of FITC-dextran labeling of CNV for quantifying pharmacologic intervention, we examined the effect of dexamethasone, a proven angiostatic corticosteroid, on CNV as measured by FITC-dextran labeling and Factor VIII immunostaining. Figs 2 and 3 show that the extent of CNV reaches its maximum by day 10, and therefore, this time-point was selected as optimal for measuring drug effect.

Fig. 7 shows the effect of dexamethasone ($20-500 \mu g \ kg^{-1} \ day^{-1}$ by oral gavage) on experimental CNV measured in flat mounts 10 days after lasering. Dexamethasone inhibited CNV by 48% at $20 \mu g \ kg^{-1} \ day^{-1}$, by 64% at $100 \mu g \ kg^{-1} \ day^{-1}$, and by 95% at $500 \mu g \ kg^{-1} \ day^{-1}$. A representative lesion from the high dose dexamethasone group ($500 \mu g \ kg^{-1} \ day^{-1}$) is shown in Fig. 8(B). The lesion is hypofluorescent and devoid of new blood vessels. Factor VIII immunostaining in histologic sections [Fig. 8(D)] supports this observation and shows that this dose of dexamethasone inhibited the development of an organized lesion and the invasion of vascular endothelial cells.

4. Discussion

Choroidal neovascularization (CNV) is associated with a change in the normal function of Bruch's membrane and retinal pigment epithelium (RPE) and causes severe vision loss in patients with age-related macular degeneration (ARMD). As first reported by Ryan (1979), laser-induced disruption of the RPE and Bruch's membrane in primates results in
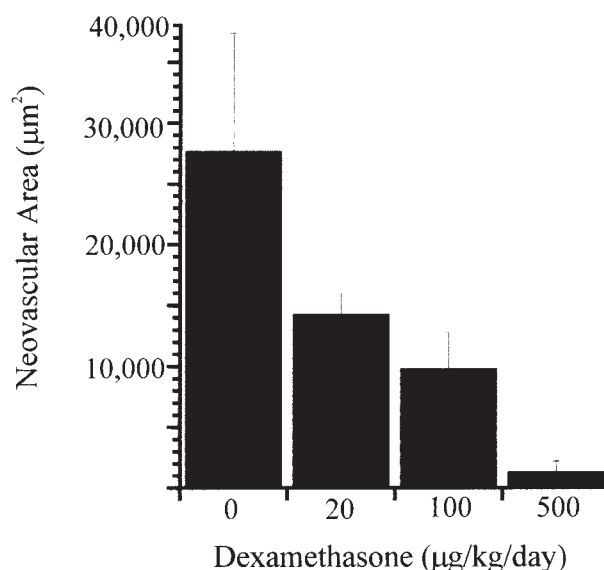

FIG. 7. Dose-dependent inhibition of CNV by dexamethasone. Neovascular area was measured by quantitative digital image analysis of FITC-dextran labeled RPE-choroid-sclera flat mounts. Dexamethasone was suspended in corn oil, and rats were dosed daily by oral gavage. Values are mean ± S.D. for three rats per group receiving dexamethasone, and seven rats in the control group. There is a significant difference between neovascularization in the control group and that of all groups treated with dexamethasone ($P < 0.05$; Bonferroni multiple comparison test).

subretinal neovascular lesions that leak fluorescein in angiography and show remarkable similarity to lesions in ARMD patients. This method of inducing CNV by laser was subsequently developed in rodents, and blood vessel growth was characterized by angiography, histology, and vascular casting in these models (Dobi et al., 1989; Frank et al., 1989; Seo et al., 1999). Rodent models of laser-induced CNV are now extensively used to identify angiogenic proteins (e.g. Nishimura et al., 1990), determine the role of specific genes with knockout mice (Tobe et al., 1998), and evaluate the efficacy of anti-angiogenic therapies (e.g. Seo et al., 1999).

The first goal of the current study was to develop an alternative method to measure blood vessel growth in a rat model of experimental CNV. Since high molecular weight FITC-dextran was successfully used for angiography in mouse retinal flat mounts (D'Amato et al., 1993; Smith et al., 1994), we employed a similar strategy to label and measure CNV in RPE-choroid-sclera flat mounts after laser photocoagulation. Combined with H & E and Factor VIII immunostaining is histologic sections, our results clearly establish the temporal and spatial development of functional blood vessels within the lesion after laser photocoagulation. At 3 days after lasering, there is negligible FITC-dextran labeling within lesions, and this parallels the immunohistologic finding that Factor-VIII-positive vascular endothelial cells invade the lesion at this time but do not form a functional
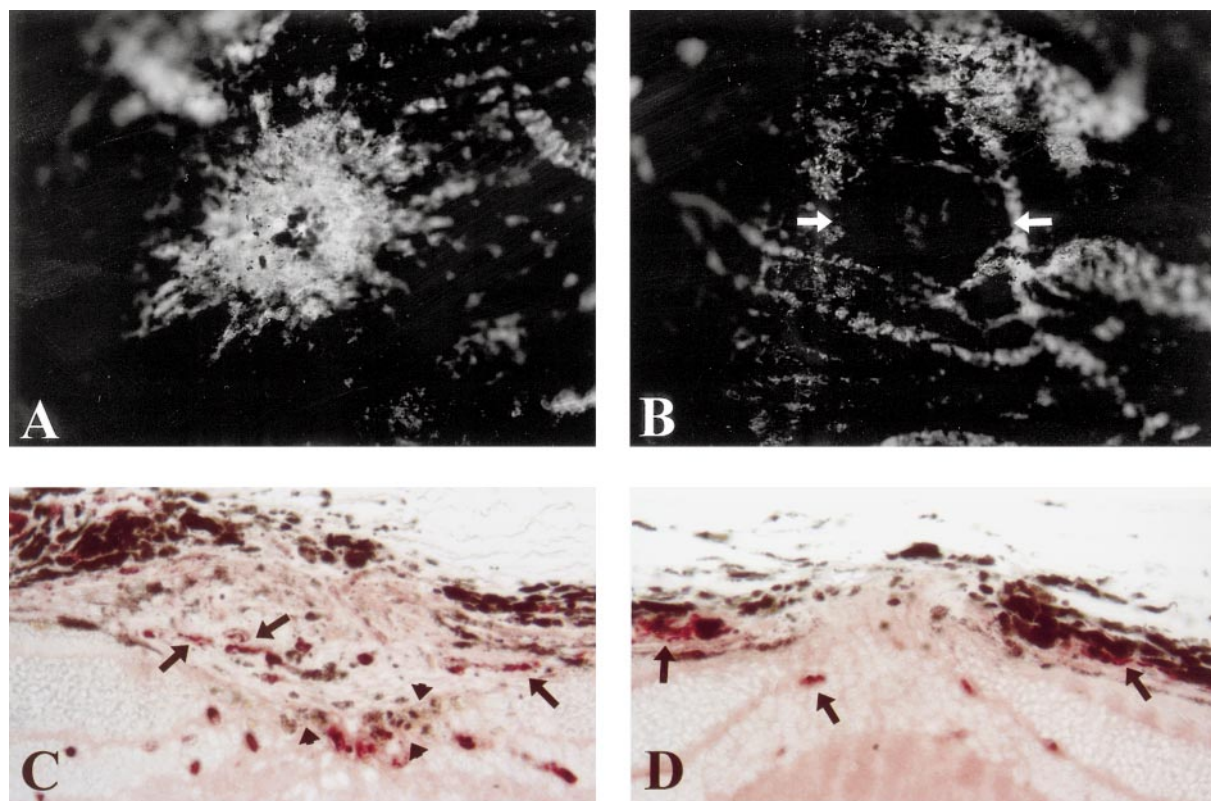
FɪG. 8. Dexamethasone (500 μg kg^{-1} day^{-1}, p.o.) markedly suppresses CNV as seen in either FITC-dextran labeled flat mounts or Factor VIII immunohistologic sections. (A) FITC-dextran labeling of CNV in untreated rats at day 10. (B) Rats treated with dexamethasone for 10 days show negligible FITC-dextran labeling within the lesion. The border of the hypofluorescent lesion is denoted by the white arrows. Uninjured, perfusing vessels surround the lesion. (C, D) Factor VIII immunostaining of vascular endothelial cells in cross sections from control (C; $n = 6$) and dexamethasone-treated (D; $n = 6$) rats 10 days after lasering. The arrows in (C) denote Factor VIII-positive vascular endothelial cells within the lesion. The arrowheads in (C) denote melanin-laden macrophages at the border of the lesion and neural retina. Arrows in (D) denote Factor VIII-positive vascular endothelial cells in the outer plexiform layer of the retina, and also in the choroid and choriocapillaris.

neovascular plexus. By day 6, the incidence and extent of FITC-dextran labeling within lesions significantly increase, and blood vessels lined with Factor VIII-positive cells are clearly seen in cross section. Results from flat mounts and cross sections at this time indicate that the neovascular net is derived from deeper choroidal vessels that branch radially in the center of the lesion towards the neural retina, and then laterally and posteriorly towards uninjured choriocapillaris. The radial, anterior growth may be driven by pigment laden cells, presumably macrophages, that are common at this time in the subretinal space in the center of the lesion (Figs 5 and 6). By day 10, the neovascular plexus in flat mounts reaches its maximal size and density, and most lesions contain broad, flat microvessels that resemble the native choriocapillaris (Dobi et al., 1989). Similarly, lesion size and blood vessel density in histologic sections are greatest at day 10 and subsequent time points.

The highest growth rate of new choroidal vessels is seen between 3 and 10 days after lasering, and this correlates temporally with increased expression of angiogenic growth factors and their receptors described by previous studies of experimental CNV in rat. For example, bFGF mRNA expression was elevated 3–7 days after lasering, and this endothelial cell mitogen was localized to several cell types within and surrounding the lesion (Ogata et al., 1996). Similarly, mRNA expression of VEGF and its receptor, VEGFR-2 (flk-1, KDR), was highest 3–7 days after lasering (Shen et al., 1993; Yi et al., 1997; Wada et al., 1999). In these studies, bFGF and VEGF/ VEGFR-2 mRNA expression significantly decreased by 2 weeks after lasering. This correlates with our results showing no further increase in the extent of CNV between days 10 and 31 after lasering.

The second goal of this study was to assess the utility of high resolution FITC-dextran angiography to measure drug efficacy. The angiostatic corticosteroid dexamethasone was selected because it markedly inhibited corneal (Proia et al., 1993; Edelman, Castro and Wen, 1999) and retinal (Rotschild et al., 1999) neovascularization in rodents, and choroidal neovascularization in primates (Ishibashi et al., 1985). Our results show that dexamethasone dose-dependently inhibited CNV, and its highest dose (500 μg kg^{-1} day^{-1}) nearly completely inhibited blood vessel formation measured by FITC-dextran fluorescence in flat mounts. This finding was supported by Factor VIII immunohistochemistry

which showed that dexamethasone inhibited the formation of a defined cellular lesion and invasion of vascular endothelial cells.

The cellular mechanism(s) by which dexamethasone represses CNV is unclear. One possibility is that dexamethasone indirectly inhibits neovascularization by suppressing the recruitment or altering the function of macrophages or other pro-angiogenic inflammatory cells (Anstead, 1998). Alternatively, dexamethasone may directly affect blood vessel growth as is suggested by its efficacy in a model of retinal neovascularization which lacks an obvious inflammatory component (Rotschild et al., 1999). Supporting this, dexamethasone inhibits VEGF production in cultured cells (Nauck et al., 1997) and in vivo (Edelman et al., 1999), and it reduces capillary-like tube formation and urokinase-type plasminogen activator expression in microvascular endothelial cells (Lansink et al., 1998). Further studies are required, however, to clarify which of these dexamethasone-sensitive mechanisms underlie the marked inhibition of laser-induced CNV.

Several therapeutic strategies, including a related corticosteroid, triamcinolone, are being tested to treat neovascular ARMD (Challa et al., 1998). These are anticipated to replace laser photocoagulation of CNV, which is only performed on a limited number of ARMD patients that show a clearly defined neovascular lesion (Lee et al., 1998). For the majority of patients, no accepted treatment for preserving central vision is available. Photodynamic therapy uses targeted laser activation of photosensitive dyes to selectively ablate or close choroidal vessels (Schmidt-Erfurth et al., 1999), and this therapy may soon be the standard of care for a limited group of ARMD patients. Small molecule inhibitors of angiogenesis are being developed to treat neovascular ARMD (Ishida et al., 1999; McNatt et al., 1999; Seo et al., 1999), and these may be useful for treating a larger population of patients in the future. The method of FITC-dextran labeling of CNV described in this study is reproducible and quantifiable, and it may accelerate the discovery of therapeutic interventions to treat choroidal neovascularization.

References

Anstead, G. M. (1998). Steroids, retinoids, and wound healing. *Adv. Wound. Care* 11, 277–85.

Challa, J. K., Gillies, M. C., Penfold, P. L., Gyory, J. F., Hunyor, A. B. and Billson, F. A. (1998). Exudative macular degeneration and intravitreal triamcinolone: 18 month follow up. *Aust. N.Z. J. Ophthalmol.* 26, 277–81.

D'Amato, R., Wesolowski, E. and Smith, L. E. (1993). Microscopic visualization of the retina by angiography with high-molecular-weight fluorescein-labeled dextrans in the mouse. *Microvasc. Res.* 46, 135–42.

D'Amico, D. J. (1994). Diseases of the retina. *N. Engl. J. Med.* 331, 95–106.

Dobi, E. T., Puliafito, C. A. and Destro, M. (1989). A new model of experimental choroidal neovascularization in the rat. *Arch. Ophthalmol.* 107, 264–9.

Edelman, J. L., Castro, M. R. and Wen, Y. (1999). Correlation of VEGF expression by leukocytes with the growth and regression of blood vessels in the rat cornea. *Invest. Ophthalmol. Vis. Sci.* 40, 1112–23.

Frank, R. N., Das, A. and Weber, M. L. (1989). A model of subretinal neovascularization in the pigmented rat. *Curr. Eye Res.* 8, 239–47.

Ishibashi, T., Hata, Y., Yoshikawa, H., Nakagawa, K., Sueishi, K. and Inomata, H. (1997). Expression of vascular endothelial growth factor in experimental choroidal neovascularization. *Graefes Arch. Clin. Exp. Ophthalmol.* 235, 159–67.

Ishibashi, T., Inomata, H., Sakamoto, T. and Ryan, S. J. (1995). Pericytes of newly formed vessels in experimental subretinal neovascularization. *Arch. Ophthalmol.* 113, 227–31.

Ishibashi, T., Miki, K., Sorgente, N., Patterson, R. and Ryan, S. J. (1985). Effects of intravitreal administration of steroids on experimental subretinal neovascularization in the subhuman primate. *Arch. Ophthalmol.* 103, 708–11.

Ishida, K., Yoshimura, N., Mandai, M. and Honda, Y. (1999). Inhibitory effect of TNP-470 on experimental choroidal neovascularization in a rat model. *Invest. Ophthalmol. Vis. Sci.* 40, 1512–9.

Lansink, M., Koolwijk, P., van Hinsbergh, V. and Kooistra, T. (1998). Effect of steroid hormones and retinoids on the formation of capillary-like tubular structures of human microvascular endothelial cells in fibrin matrices is related to urokinase expression. *Blood* 92, 927–38.

Lee, P., Wang, C. C. and Adamis, A. P. (1998). Ocular neovascularization: an epidemiologic review. *Surv. Ophthalmol.* 43, 245–69.

McNatt, L. G., Weimer, L., Yanni, J. and Clark, A. F. (1999). Angiostatic activity of steroids in the chick embryo CAM and rabbit cornea models of neovascularization. *J. Ocul. Pharmacol. Ther.* 15, 413–23.

Miller, H., Miller, B., Ishibashi, T. and Ryan, S. J. (1990). Pathogenesis of laser-induced choroidal subretinal neovascularization. *Invest. Ophthalmol. Vis. Sci.* 31, 899–908.

Miller, J. W., Walsh, A. W., Kramer, M., Hasan, T., Michaud, N., Flotte, T. J., Haimovici, R. and Gragoudas, E. S. (1995). Photodynamic therapy of experimental choroidal neovascularization using lipoprotein-delivered benzoporphyrin. *Arch. Ophthalmol.* 113, 810–8.

Nauck, M., Roth, M., Tamm, M., Eickelberg, O., Wieland, H., Stulz, P. and Perruchoud, A. P. (1997). Induction of vascular endothelial growth factor by platelet-activating factor and platelet-derived growth factor is down-regulated by corticosteroids. *Am. J. Respir. Cell Mol. Biol.* 16, 398–406.

Nishimura, T., Goodnight, R., Prendergast, R. A. and Ryan, S. J. (1990). Activated macrophages in experimental subretinal neovascularization. *Ophthalmologica* 200, 39–44.

Ogata, N., Matsushima, M., Takada, Y., Tobe, T., Takahashi, K., Yi, X., Yamamoto, C., Yamada, H. and Uyama, M. (1996). Expression of basic fibroblast growth factor mRNA in developing choroidal neovascularization. *Curr. Eye Res.* 15, 1008–18.

Ogata, N., Yamamoto, C., Miyashiro, M., Yamada, H., Matsushima, M. and Uyama, M. (1997). Expression of transforming growth factor-beta mRNA in experimental choroidal neovascularization. *Curr. Eye Res.* 16, 9–18.

Ohkuma, H. and Ryan, S. J. (1983). Vascular casts of experimental subretinal neovascularization in monkeys. *Invest. Ophthalmol. Vis. Sci.* **24**, 481–90.

Proia, A. D., Harakata, A., McInnes, J. S., Scroggs, M. W. and Parikh, I. (1993). The effect of angiostatic steroids and beta-cylodextrin tetradecasulfate on corneal neovascularization in the rat. *Exp. Eye Res.* **57**, 693–8.

Rotschild, T., Nandgaonkar, B. N., Yu, K. and Higgins, R. D. (1999). Dexamethasone reduces oxygen induced retinopathy in a mouse model. *Pediatr. Res.* **46**, 94–100.

Ryan, S. J. (1979). The development of an experimental model of subretinal neovascularization in disciform macular degeneration. *Trans. Am. Ophthalmol. Soc.* **77**, 707–45.

Schmidt-Erfurth, U., Miller, J. W., Sickenberg, M., Laqua, H., Barbazetto, I., Gragoudas, E. S., Zografos, L., Piguet, B., Pournaras, C. J., Donati, G., Lane, A. M., Birngruber, R., van den, B. H., Strong, H. A., Manjuris, U., Gray, T., Fsadni, M. and Bressler, N. M. (1999). Photodynamic therapy with verteporfin for choroidal neovascularization caused by age-related macular degeneration: results for retreatments in a phase 1 and 2 study [comment] [see comments]. *Arch. Ophthalmol.* **117**, 1177–87.

Seo, M. S., Kwak, N., Ozaki, H., Yamada, H., Okamoto, N., Yamada, E., Fabbro, D., Hofmann, F., Wood, J. M. and Campochiaro, P. A. (1999). Dramatic inhibition of retinal and choroidal neovascularization by oral administration of a kinase inhibitor. *Am. J. Pathol.* **154**, 1743–53.

Shen, H., Clauss, M., Ryan, J., Schmidt, A. M., Tijburg, P., Borden, L., Connolly, D., Stern, D. and Kao, J. (1993). Characterization of vascular permeability factor/ vascular endothelial growth factor receptors on mononuclear phagocytes. *Blood* **81**, 2767–73.

Smith, L. E., Wesolowski, E., McLellan, A., Kostyk, S. K., D'Amato, R., Sullivan, R. and D'Amore, P. A. (1994). Oxygen-induced retinopathy in the mouse. *Invest. Ophthalmol. Vis. Sci.* **35**, 101–11.

Takehana, Y., Kurokawa, T., Kitamura, T., Tsukahara, Y., Akahane, S., Kitazawa, M. and Yoshimura, N. (1999). Suppression of laser-induced choroidal neovascularization by oral tranilast in the rat. *Invest. Ophthalmol. Vis. Sci.* **40**, 459–66.

Tobe, T., Ortega, S., Luna, J. D., Ozaki, H., Okamoto, N., Derevjanik, N. L., Vinores, S. A., Basilico, C. and Campochiaro, P. A. (1998). Targeted disruption of the FGF2 gene does not prevent choroidal neovascularization in a murine model. *Am. J. Pathol.* **153**, 1641–6.

Wada, M., Ogata, N., Otsuji, T. and Uyama, M. (1999). Expression of vascular endothelial growth factor and its receptor (KDR/flk-1) mRNA in experimental choroidal neovascularization. *Curr. Eye Res.* **18**, 203–13.

Yi, X., Ogata, N., Komada, M., Yamamoto, C., Takahashi, K., Omori, K. and Uyama, M. (1997). Vascular endothelial growth factor expression in choroidal neovascularization in rats. *Graefes Arch. Clin. Exp. Ophthalmol.* **235**, 313–9.

Yi, X., Takahashi, K., Ogata, N. and Uyama, M. (1996). Immunohistochemical proof of origin of macrophages in laser photocoagulation lesion in the retina. *Jpn. J. Ophthalmol.* **40**, 192–201.

Zhang, N. L., Samadani, E. E. and Frank, R. N. (1993). Mitogenesis and retinal pigment epithelial cell antigen expression in the rat after krypton laser photocoagulation. *Invest. Ophthalmol. Vis. Sci.* **34**, 2412–24.